

Structural Analysis of Alkaline β -Mannanase from Alkaliphilic *Bacillus* sp. N16-5: Implications for Adaptation to Alkaline Conditions

Yueju Zhao^{1,2}, Yunhua Zhang¹, Yang Cao^{2,3}, Jianxun Qi⁴, Liangwei Mao⁵, Yanfen Xue¹, Feng Gao⁴, Hao Peng⁴, Xiaowei Wang¹, George F. Gao⁴, Yanhe Ma^{1*}

1 State Key Laboratory of Microbial Resources, Institute of Microbiology, Chinese Academy of Sciences, Beijing, People's Republic of China, **2** Graduate University, Chinese Academy of Sciences, Beijing, People's Republic of China, **3** National Laboratory of Biomacromolecules, Institute of Biophysics, Chinese Academy of Sciences, Beijing, People's Republic of China, **4** Key Laboratory of Pathogenic Microbiology and Immunology, Institute of Microbiology, Chinese Academy of Sciences, Beijing, People's Republic of China, **5** College of Life Science, Hubei University, Wuhan, People's Republic of China

Abstract

Significant progress has been made in isolating novel alkaline β -mannanases, however, there is a paucity of information concerning the structural basis for alkaline tolerance displayed by these β -mannanases. We report the catalytic domain structure of an industrially important β -mannanase from the alkaliphilic *Bacillus* sp. N16-5 (BSP165 MAN) at a resolution of 1.6 Å. This enzyme, classified into subfamily 8 in glycosyl hydrolase family 5 (GH5), has a pH optimum of enzymatic activity at pH 9.5 and folds into a classic $(\beta/\alpha)_8$ -barrel. In order to gain insight into molecular features for alkaline adaptation, we compared BSP165 MAN with previously reported GH5 β -mannanases. It was revealed that BSP165 MAN and other subfamily 8 β -mannanases have significantly increased hydrophobic and Arg residues content and decreased polar residues, comparing to β -mannanases of subfamily 7 or 10 in GH5 which display optimum activities at lower pH. Further, extensive structural comparisons show alkaline β -mannanases possess a set of distinctive features. Position and length of some helices, strands and loops of the TIM barrel structures are changed, which contributes, to a certain degree, to the distinctly different shaped $(\beta/\alpha)_8$ -barrels, thus affecting the catalytic environment of these enzymes. The number of negatively charged residues is increased on the molecular surface, and fewer polar residues are exposed to the solvent. Two amino acid substitutions in the vicinity of the acid/base catalyst were proposed to be possibly responsible for the variation in pH optimum of these homologous enzymes in subfamily 8 of GH5, identified by sequence homology analysis and pK_a calculations of the active site residues. Mutational analysis has proved that Gln91 and Glu226 are important for BSP165 MAN to function at high pH. These findings are proposed to be possible factors implicated in the alkaline adaptation of GH5 β -mannanases and will help to further understanding of alkaline adaptation mechanism.

Citation: Zhao Y, Zhang Y, Cao Y, Qi J, Mao L, et al. (2011) Structural Analysis of Alkaline β -Mannanase from Alkaliphilic *Bacillus* sp. N16-5: Implications for Adaptation to Alkaline Conditions. PLoS ONE 6(1): e14608. doi:10.1371/journal.pone.0014608

Editor: Shuang-yong Xu, New England Biolabs, Inc, United States of America

Received: July 13, 2010; **Accepted:** January 4, 2011; **Published:** January 28, 2011

Copyright: © 2011 Zhao et al. This is an open-access article distributed under the terms of the Creative Commons Attribution License, which permits unrestricted use, distribution, and reproduction in any medium, provided the original author and source are credited.

Funding: This work was supported by grants from the National Natural Science Foundation of China (NSFC: 30621005) and from the Ministry of Sciences and Technology of China (973 programs 2007CB707801 and 2003CB716001, 863 programs 2006 AA020201 and 2007AA021306). The funders had no role in study design, data collection and analysis, decision to publish, or preparation of the manuscript.

Competing Interests: The authors have declared that no competing interests exist.

* E-mail: mayanhe@im.ac.cn

Introduction

Alkaline enzymes show great advantages of functioning under alkaline conditions during the industrial application process as biotransformation catalysts and offer an attractive opportunity for investigating adaptation mechanisms in extreme high pH conditions. Significant progress has been made in isolating novel alkaline enzymes [1], [2], [3], however, their underlying alkaline adaptation mechanisms have not been studied sufficiently.

Beta-mannanases (EC 3.2.1.78) randomly hydrolyze the β -1,4-mannosidic linkages in mannan and heteromannan [4], [5] and these enzymes have great potential uses in the food, paper and detergent industries [6], [7]. Alkaline β -mannanases are capable of functioning under the alkaline conditions during the manufacture of kraft paper and in the detergent industry. Therefore, the discovery of β -mannanases that are stable at alkaline pH has aroused industrial interest. Several alkaline β -mannanases from

the alkaliphilic microorganisms *Bacillus* sp. strains AM001, JAMB602, JAMB750, I633 and N16-5, *Bacillus circulans* strains CGMCC1554 and CGMCC1416 and *Bacillus agaradhaerens*, have been characterized and classified into glycosyl hydrolase (GH) families 5 and 26 [8], [9], [10], [11], [12], [13], [14]. In addition, the tertiary structures have been solved for β -mannanases from alkaliphilic *Bacillus* sp. JAMB602 (PDB code 1WKY) [10] and *Bacillus agaradhaerens* (PDB code 2WHJ) [15]. However, there is a paucity of information concerning the structural basis for the alkaline tolerance displayed by β -mannanases.

Of all the characterized alkaline β -mannanases, the one from *Bacillus* sp. strain N16-5 (BSP165 MAN) has stimulated great interest. This enzyme not only shows a pH optimum as high as 9.5 but also has a high specific activity of 5065 U/mg. These properties, combined with its characteristics of stability under alkaline conditions and insensitivity to some surfactants, would qualify the mannanase as a candidate in the manufacture of kraft

pulp and in the detergent industry. The catalytic domain of BSP165 MAN, which shows virtually the same pH activity profile and specific activity as the full-length enzyme, has been expressed, purified and crystallized and preliminary X-ray studies have been performed [16]. Solving the three-dimensional structure of BSP165 MAN would help to decipher the structural basis for alkaline adaptation of the GH5 β -mannanases.

Here, we report the crystal structure of the catalytic domain of BSP165 MAN. To investigate the distinct structural features linked to alkaline adaptation, we carried out a comprehensive comparative analysis of BSP165 MAN with other family 5 mannanases. This is the first report to investigate the basis of alkaline adaptation of β -mannanases. These findings will not only deepen our understanding of adaptation mechanism of proteins to alkaline conditions, but will also help in the optimization of the pH-dependent characteristics of enzymes for a broad range of industrial applications.

Results

Structure determination of the β -mannanase from *Bacillus* sp. strain N16-5

The crystal structure of the catalytic domain of BSP165 MAN has been determined at a resolution of 1.6 Å by molecular replacement using the coordinates of alkaliphilic *Bacillus* sp. JAMB-602 β -mannanase (PDB code, 1WKY; sequence identity, 78%) [10], which also belongs to the GH subfamily 5–8, as a search model. Refinement of BSP165 MAN at a resolution of 1.6 Å resulted in an electron density map of excellent quality for the majority of the residues. However, weak electron density was obtained for a number of highly mobile side chains on the solvent exposed molecular surface. Residues 260 and 261 were not modeled due to lack of sufficient electron density data and, hence, are not included in the refinement. Asp65 has two possible conformations and the side chain of Asp65 seems to have considerable mobility based on the electron density map.

Towards the end of the refinement, water molecules were evident in the electron density maps and were included in the model. One peak of tetrahedral geometry was interpreted as SO_4^{2-} , based on the 2Fo-Fc map contoured at 2 σ and their presence in the crystallization medium.

The final model, consisting of 295 amino acid residues, has a crystallographic R-factor of 17.4% and an R-free value of 21.5%. A Ramachandran plot confirmed the stereochemical validity where all residues are in allowed regions with acceptable values of bond angle geometry. Details of the refinement and stereochemistry of the final model are provided in Table 1.

Overall structure of the β -mannanase from *Bacillus* sp. strain N16-5

The crystal structure of the catalytic domain of BSP165 MAN adopts the canonical $(\beta/\alpha)_8$ -barrel architecture. It is composed of ten β -strands and thirteen α -helices including three 3_{10} -helices (residue 60–62, 64–66 and 289–294). The β -sheet structures consisting of eight parallel β -strands (yellow) lie in the middle forming a barrel surrounded by eight α -helices (red) with a size of $45 \times 45 \times 40 \text{ \AA}^3$. Aside from the structural elements of the barrel, two short β -strands (yellow) at the N terminus form the bottom of the barrel (Figure 1). Additional secondary structures including two α -helices (cyan) and three 3_{10} -helices (blue) are on the bottom and top of barrel, respectively.

Comparison with other Family 5 β -mannanases

Amino acid sequences of 30 family 5 β -mannanases reported in literature with known pH-dependent activity were retrieved.

Table 1. Crystal parameters and refinement quality statistics.

Parameters	BSP165 MAN
Crystallographic data	
Space group	P2 ₁ 2 ₁ 2 ₁
Cell parameters (Å, °)	a = 59.0, b = 63.3, c = 83.3, $\alpha = \beta = \gamma = 90$
Data collection	
Resolution range (Å)	63.29 – 1.60 (1.71– 1.60)
Total number of reflections	182424(7471)
Number of unique reflections	38945(4841)
Average redundancy	4.68 (1.54)
Completeness (%)	92.74 (65.44)
R _{sym} (%) ^a	7.6 (40.7)
Average I/ σ (I)	7.63 (1.95)
Refinement	
R _{factor} /R _{free} (%)	17.4/21.5
No. of all protein atoms	2315
Mean B-values (Å ²)	6.9
No. of SO ₄ atoms	5
Mean B-values (Å ²)	17.5
No. of water molecules	579
Mean B-values (Å ²)	25.3
RMSD bonds (Å ²)	0.007
RMSD angles (°)	1.1
Ramachandran Plot %-residue in the most favored region ^b	89.5%
%-residue in additional allowed region	10.2%
%-residue in generously allowed region	0.4%
%-residue in disallowed region	0
PDB code	3JUG

Values in parentheses correspond to the highest resolution shell.

^aR_{sym} = $\sum_{\mathbf{h}} \sum_i |I_i(\mathbf{h}) - \langle I(\mathbf{h}) \rangle| / \sum_{\mathbf{h}} \sum_i \langle I(\mathbf{h}) \rangle$, where $I_i(\mathbf{h})$ is the i th observation of reflection \mathbf{h} and $\langle I(\mathbf{h}) \rangle$ is the weighted average intensity for all observations i of reflection \mathbf{h} .

^bCalculated for nonglycine and nonproline residues using PROCHECK.

doi:10.1371/journal.pone.0014608.t001

Besides structure of BSP165 MAN, 3D structures have been solved for other 5 enzymes (BA MAN, *Bacillus agaradhaerens* β -mannanase; BSP602 MAN, *Bacillus* sp. JAMB-602 β -mannanase; TF MAN, *Thermomonospora fusca* β -mannanase; ME MAN, *Mytilus edulis* β -mannanase; HJ MAN, *Hypocrea jecorina* RUTC-30 β -mannanase in Table S1). The molecular phylogeny of these enzymes is shown in Figure S1. Major branches form two clusters: cluster A which is composed of 13 bacterial β -mannanases classified into subfamily 5–8 and cluster B which includes 17 β -mannanases mainly from eukaryota, classified into subfamily 5–7 and 5–10. Alkaline mannanases, BSP165 MAN and its close homologues (BA, BSP602, BC15554 and BC1416 MAN), all belong to subfamily 5–8 in cluster A, while most of mannanases of cluster B act at acidic pH.

Total amino acid composition of family 5 β -mannanases

A thorough comparison of enzymes from cluster A (classified into GH5-8) with those from cluster B (grouped into GH5-7 and GH5-10) was carried out (Table 2). The differences were assessed with the Student's t-value (a negative sign was added to the value if

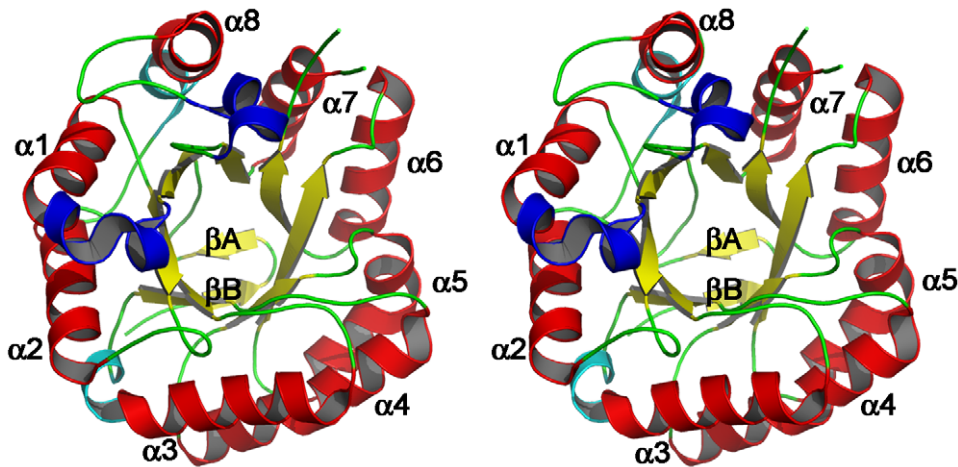


Figure 1. Overall structure of BSP165 MAN from the top view. Major α -helices and β -strands are drawn in red and yellow, respectively, and labeled according to the ideal $(\beta/\alpha)_8$ barrel structure. Two short β -strands at the N terminus are colored in yellow, and additional two α -helices and three 3_{10} -helices are in cyan and blue, respectively.
doi:10.1371/journal.pone.0014608.g001

the average is smaller for GH5-8 enzymes). Distinct difference in pH optimum was observed, indicating that β -mannanases of GH5-8 are active at higher pH than those of GH5-7 and GH5-10.

Alteration of amino acid composition is considered to relate to protein adaptation to extreme environments, so we further compared the amino acid compositions within catalytic domains of enzymes from the two clusters. The most significant differences between the two groups were the increase in hydrophobic residues and Ile contents, and decrease in Phe contents (amino acid contents-Hydrophobic, Ile and Phe in Table 2, $P=0.000$, respectively). Reductions in polar residues, Cys, Pro, Thr and Tyr contents and increase in Arg and Val contents were also observed as significant events (amino acid contents-Polar, Cys, Pro, Thr, Tyr, Arg and Val in Table 2, $P=0.011$, 0.001, 0.022, 0.003, 0.001, 0.008 and 0.004). These findings indicate increasing the relative frequency of hydrophobic residues and Arg residue as well as decreasing that of polar residues could relate to an increase in the optimum pH for the enzyme activity.

Structure comparison of characterized Family 5 β -mannanases

In order to understand the structural basis for alkaline stability, the tertiary structures of BSP165 MAN (PDB code 3jug, optimum pH 9.5) and its close homologues, BA (PDB code 2whj, optimum pH 8–10)[15] and BSP602 MAN (PDB code 1wky, optimum pH 9), have been compared with those of three other family 5 β -mannanases with known 3D structures and characterized to be active at neutral or acidic pH (TF MAN, PDB code 1bqc, optimum pH 6–8[17]; ME MAN, PDB code 2c0h, optimum pH 5.2[18], [19]; HJ MAN, PDB code 1qno, optimum pH 3.5–4[20], [21]) (Table S1).

Secondary structure

The secondary structure compositions are similar in all of the six GH5 family β -mannanases (Table S2). Figure 2 reveals that the secondary structures of the other two alkaline β -mannanases (BA and BSP602 MAN) are the most similar to that of BSP165 MAN, followed by neutral TF MAN and acidic enzymes (ME and HJ MAN).

Compared with the neutrophilic TF MAN enzyme, the alkaline β -mannanases (BSP165, BA and BSP602 MAN) show slight

differences in secondary structures. Residues from the randomly coiled loop connecting $\beta 1\alpha 1$ in TF MAN form two 3_{10} helices in alkaline β -mannanases. Loops 119–121, 162–165 and 226–228 (according to the sequence of BSP165 MAN) in these alkaline enzymes are substituted by short α -helices (residues 86–88, 134–137 and 199–201) at the corresponding regions in TF MAN.

Comparing to the ME MAN and HJ MAN, alkaline and neutral β -mannanases have two but not three β -strands at the N-terminal end of the sequence forming a motif to cap the barrel, and the loops connecting the $\alpha\beta$ -repeats are, in general, shorter with less extra short β -strands and 3_{10} -helices formed. Besides, they show obvious differences in the length of the main secondary structural elements.

Altogether, different shapes of TIM-barrels are presented (Figure S2).

Comparison of hydrogen bonds and ion pairs

In this study, changes in the number of ion pairs and hydrogen bonds were detected in the β -mannanases and the relationship between these changes and alkaline adaptation was investigated (Table S2). Similar content of ion pairs and hydrogen bonds were observed, indicating their changes may not involve in alkaline adaptation of these GH5 β -mannanases.

Protein surface comparison

Changes in amino acid content on the solvent-accessible surface were detected to check whether any correlation with alkaline adaptation can be found in these six β -mannanases. The results are presented in Table 3. The percentage of solvent-exposed negatively charged residues (Asp and Glu) is higher for alkaline-stable β -mannanases than for neutrophilic and acid-stable β -mannanases, which results in a higher ratio of negatively to positively charged residues. At the same time, the percentage of polar residues (Asn, Gln, His, Thr and Ser), especially that of easily-decomposed residues (Ser and Thr), is reduced in alkaline β -mannanases. Besides, BSP165 and BA MAN contain lower number of Asn and Gln residues that are alkaline-susceptible (Asn+Gln in Table 3, 14.3% and 14.5%, respectively), when compared with the other four mannanases active at lower pH (Asn+Gln for BSP602, TF, ME and HJ MAN in Table 3, 23.2%, 24.5%, 23.8% and 32.4%, respectively).

Table 2. Molecular features comparison of family 5 β -mannanases grouped into different phylogenetic clusters.

Parameters	Mean		t-value	P
	Cluster A	Cluster B		
pH	7.365	5.0441	4.274	0.000
p _{lcalc}	5.0577	5.3047	-0.784	0.439
Mw	27.7738	33.8341	-3.800	0.001
Ala (%)	9.6762	8.2924	2.561	0.16
Cys (%)	0.3392	1.1541	-3.563	0.001
Asp (%)	7.4938	6.4871	1.381	0.178
Glu (%)	4.7523	4.2018	1.052	0.302
Phe (%)	2.4531	3.8906	-5.025	0.000
Gly (%)	9.3115	9.4806	-0.332	0.742
His (%)	2.6131	2.4888	0.349	0.730
Ile (%)	7.1185	5.2129	4.330	0.000
Lys (%)	3.9623	4.9459	-1.291	0.212
Leu (%)	6.0323	6.4294	-0.867	0.393
Met (%)	1.9377	2.0371	-0.314	0.756
Asn (%)	7.8969	6.8153	1.650	0.110
Pro (%)	2.4338	3.1929	-2.424	0.022
Gln (%)	3.2785	3.5076	-0.611	0.546
Arg (%)	3.4154	2.1576	2.846	0.008
Ser (%)	6.5146	7.2935	-0.977	0.337
Thr (%)	5.3208	7.1341	-3.271	0.003
Val (%)	7.2915	6.0935	3.094	0.004
Trp (%)	3.7269	3.5029	1.096	0.282
Tyr (%)	4.4315	5.6829	-3.658	0.001
Charged (RKHYCDE) (%)	27.0077	27.1182	-0.072	0.943
Acidic (DE) (%)	12.2462	10.6888	1.593	0.122
Basic (KR) (%)	7.3777	7.1035	0.403	0.690
Polar (NCQSTY) (%)	27.7815	31.5876	-2.725	0.011
Hydrophobic (AILFWV) (%)	36.2985	33.4218	4.012	0.000
Number of total amino acid residues	251.4615	306.7647	-3.903	0.001

doi:10.1371/journal.pone.0014608.t002

Active site comparison

Similar to all other studied GH5 β -mannanases, the proton donor (Glu 158) in BSP165 MAN is located at the C-terminus of β 4 and the nucleophile (Glu 253) is located at the C-terminus of β 7[11]. Six other amino acids (Arg83, His119, Asn157, His223, Tyr225 and Trp282), located near the catalytic centre, are highly conserved in all the four family 5–8 β -mannanases (Figure S3A). Except His119, seven of the eight conserved residues are preserved in ME and HJ MAN (Figure S3, B and C).

Four structure-solved GH5-8 β -mannanases catalyze mannan under quite different pH conditions, despite sharing high sequence and structural identity. Amino acid residues within radius of 12 Å from either of the two catalytic amino acids in BSP165, BA, BSP602 and TF MAN were assessed to identify residues that play an important role in determining the pH optima of these homologous β -mannanases. The majority of the residues surrounding Glu158 and Glu253 are absolutely conserved, with the exception of several residues.

The sequences of all of the characterized β -mannanases in the GH5-8 family were aligned to illustrate the function of these different sites mentioned above in regulating the pH optima of β -mannanases, and 15 residues were supposed to be determinants of catalysis under different pH conditions (Figure 3). To evaluate this hypothesis, structures of reciprocal single-site mutants at these 15 positions around the active site of BSP165 and TF MAN in complex with mannotriose were constructed and pK_a calculations were carried out (Table 4). We define mutations that would be discernible in the pH-activity profile as mutations that give a shift of more than 0.3 pK_a units for either of the two catalytic acids. The results showed that mutations at positions corresponding to Gln-91 and Glu-226 of BSP165 MAN should give pK_a shifts that would be discernible in the pH-activity profiles for both enzymes in opposite directions as predicted. Therefore, we supposed that these two sites possibly played an important role in regulating pH optima of these homologues.

Further, we constructed 2 single (Q91R and E226G) and one double (QE to RG at position 91 and 226) point mutations to check their influence on pH regulation for BSP165 MAN. The pH-activity profiles are shown in Figure 4. Q91R decreases the activity of BSP165 MAN to about 51% of the wild-type activity and its pH-activity profile is pushed slightly towards more acidic pH values. pH-activity profiles for E226G and the double mutant have become almost flat and been shifted to more acidic pH values with optimum pH 8.5, which was lower by one unit than the optimum pH for the activity of the wild type mannanases.

The double mutant exhibited significantly reduced alkaline stability, while all the mutants had strengthened stability at pH 6–7.5 when compared to the wild-type enzyme (Figure 4C).

Discussion

Our target enzyme alkaline BSP165 MAN showed pH optimum as high as 9.5, one of the highest among all the known characterized GH5 mannanases. All these enzymes could be divided into clusters A and B based on the phylogenetic tree. Coincidentally, they displayed significantly different pH optimum.

Amino acid composition comparison

Based on previous studies, amino acid composition is considered to be correlated to protein adaptation to extreme environments. Several interesting studies have been reported on the relation of amino acid content and alkaline adaptation of enzymes[22], [23], [24], [25]. For alkaline proteases and cellulases, a decrease in the number of Asp and Lys residues and an increase in Arg, His and Gln residues were observed during the alkaline adaptation process[22], [23]. To explore the underlying mechanism of alkaline adaptation of GH5 mannanases, we analyzed the differences of amino acid composition among these two clusters.

The consensus amino acid content changes for the alkaline adaptation of proteases, cellulases and GH5 mannanases was an increase in the Arg content, whose pK_a value is generally higher, considered helpful for maintaining the local charge balance at higher pH[23].

Besides, GH5 mannanases have their own specific strategy to adapt to alkaline conditions by regulating amino acid contents. Mannanases in cluster A which are active at higher pH contain lower total number of polar residues, especially lower number of Tyr, Thr (easily decomposed) and Cys (easily oxidized), and that would result in a better stability under alkaline environment (Table 2). Meanwhile, an increase of hydrophobic residues (Ala, Ile, Leu, Phe, Trp and Val) was observed, and that would help cluster A mannanases to form more compact protein structures.

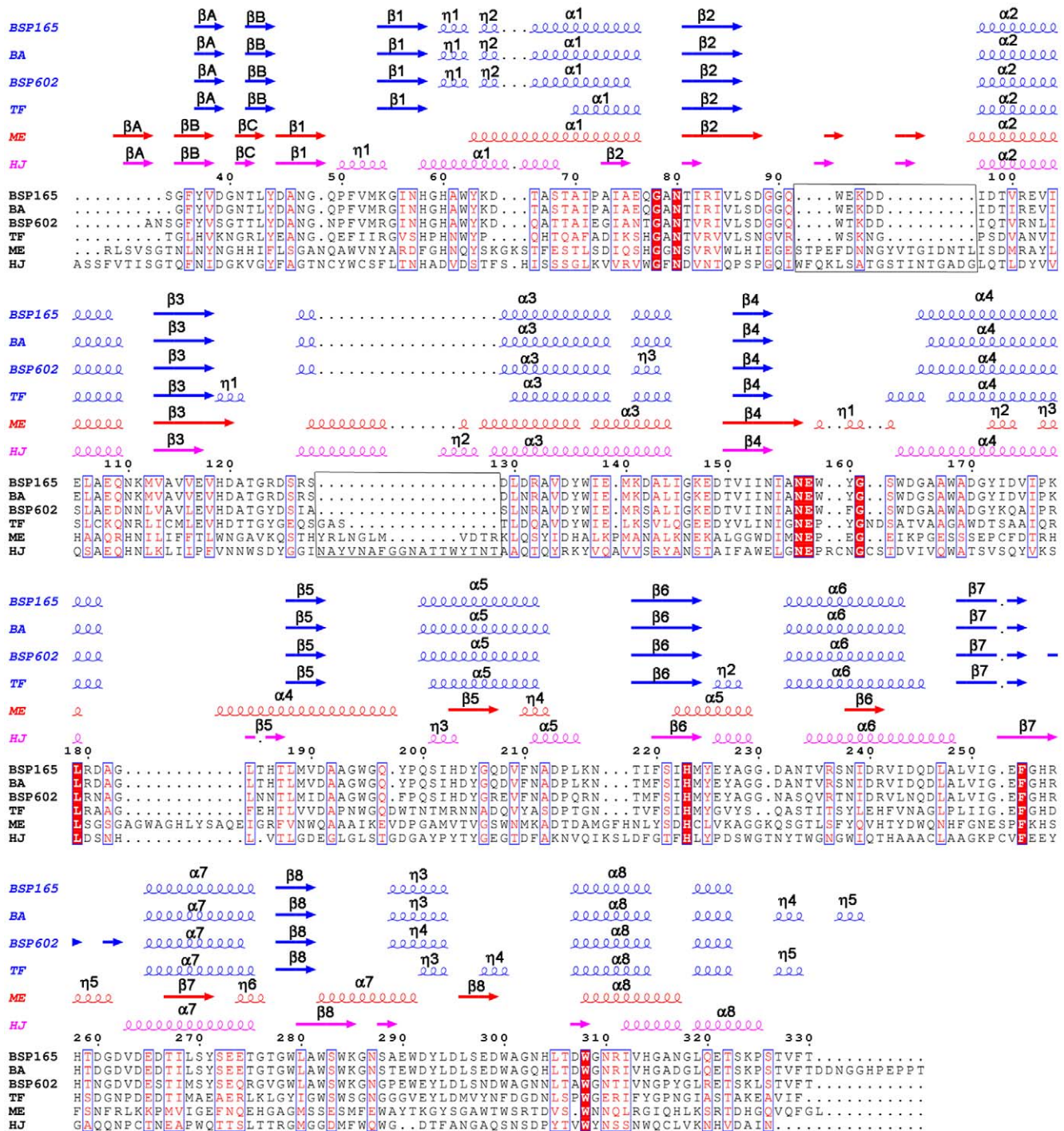


Figure 2. Structural alignment of mannanases from *Bacillus* sp. N16-5 (BSP165), *Bacillus agaradhaerens* (BA), *Bacillus* sp. strain JAMB-602 (BSP602), *Thermobifida fusca* KW3 (TF), *Hypocrea jecorina* RUTC-30 (HJ) and *Mytilus edulis* (ME). The residues are numbered as in the BSP165 MAN model. Secondary structure elements for BSP165, BA, BSP602 and TF are presented in blue, while those for HJ and ME are colored in red and magenta, respectively. The figure was produced using ESPript[55]. doi:10.1371/journal.pone.0014608.g002

We further calculated the compactness of the six structure-known mannanases active at quite different pH conditions, shown in table S2, and found a negative correlation between compactness coefficient and the optimum pH for enzyme activity (Pearson correlation coefficient = -0.906 , $P = 0.013$). It indicates a trend towards increase in compactness with an increase in optimum pH.

Thus, increased compactness may contribute to structural adaptation of mannanases to alkaline pH. No obvious differences in the number of lysine residues between these two clusters of β -mannanases were observed, although loss of lysine residues during the alkaline adaptation process of amylases, cellulases and phosphoserine aminotransferases has been observed[24]. These

Table 3. Amino acid content on the surface of GH5 β -mannanases with known 3D structure.

Parameters	BSP165	BA	BSP602	TF	ME	HJ
PDB code	3jug	2whj	1wky	1bqc	2c0h	1qno
Total	56	55	56	53	63	74
Asp (%)	23.2	25.5	14.3	7.5	4.8	5.4
Glu (%)	17.9	18.2	10.7	7.5	3.2	1.4
Negatively charged (%)	41.1	43.6	25	15.1	7.91	6.8
Arg (%)	7.1	1.8	12.5	1.9	7.94	1.4
Lys (%)	7.1	7.3	3.6	7.5	11.1	6.8
Positively charged (%)	14.3	9.1	16.1	9.41	19.0	8.1
Negatively charged/ positively charged (%)	2.9	4.8	1.6	1.6	0.4	0.8
Asn (%)	7.1	5.5	17.9	11.3	17.5	13.5
Gln (%)	7.1	9.1	5.4	13.2	6.3	18.9
His (%)	3.6	3.6	0	0	7.9	1.4
Thr (%)	1.8	7.3	3.6	3.8	4.8	16.2
Ser (%)	5.4	5.5	8.9	15.1	15.9	14.9
Polar, uncharged (%)	25	30.9	35.7	43.4	52.4	64.9
Tyr (%)	3.6	1.8	1.8	5.7	1.6	1.4
Gly (%)	0	1.8	1.8	3.8	7.9	8.1
Pro (%)	5.4	5.5	8.9	7.5	1.6	2.7
Trp (%)	5.4	5.5	1.8	1.9	3.2	0
Leu (%)	0	0	1.8	0	0	0
Ile (%)	1.8	0	1.8	0	0	0
Val (%)	0	0	0	0	3.2	0
Ala (%)	3.6	1.8	5.4	13.2	3.2	8.1
Hydrophobic (%)	19.6	16.4	23.2	32.1	20.6	20.3
Asn+Gln (%)	14.3	14.5	23.2	24.5	23.8	32.4
Thr+Ser (%)	7.2	12.8	12.5	18.9	20.7	31.1

doi:10.1371/journal.pone.0014608.t003

observations suggest that changes in the composition of amino acid residues as mechanism of alkaline adaptation might not be universal but specific for each protein.

Secondary structures

Adaptation to extreme conditions can occur in evolution within a short time in both directions by incorporation or exchange of short sequences with the appropriate physical-chemical properties without the need for gradual changes over the whole polypeptide chain[26]. When the six structure-known enzymes were aligned, two major inserted stretches >10 amino acids (Figure 2) were observed in acidic mannanases. The percentages of polar residues (easily decomposed Ser and Thr, easily oxidized Cys, alkaline susceptible Asn and Gln) in the two inserted stretches in acidic mannanases (ME and HJ MAN) are 34.5% and 44.4% respectively, much higher than that in the neutral and alkaline enzymes (29.7% in TF MAN, 24.6% in BA MAN, 27.5% in BSP602 MAN and 23.5% in BSP165 MAN). Accordingly, it is proposed that deleting stretches rich in polar residues that are easily deaminated and oxidized at alkaline pH to acquire better stability could be a means for rapid alkaline adaptation of mannanases.

Rearrangement of helices, strands and loops in the active regions caused by the secondary structural differences, contributes,

to a certain degree, to the distinctly different shaped catalytic clefts in these enzymes (Figure S2). These differences above lead to changes in the polarity, charge distribution and/or hydrogen bonding in the microenvironment of the active site of these β -mannanases, which might in turn affect the protonation state of key catalytic amino acids, and subsequently determine the pH optimum of the enzyme. Changing the microenvironment of the active site by site-directed mutagenesis has been shown to increase the pH optimum of glucoamylase from *Aspergillus awamori*[27]. Thereby we propose that reorganization of the chameleon-like TIM barrel surrounding the catalytic center of the protein could be a mechanism for adaptation to alkaline conditions.

Hydrogen bonds and ion pairs

Despite numerous previous studies[22], [23], [28], no general strategy has yet been confirmed by which an enzyme can adapt to high pH by changing the numbers of ion pairs. Strategies are generally specific for each enzyme class. In this study, for β -mannanases there is no correlation between changes in the number of ionic interactions and alkaline adaptation.

An increase of hydrogen bonds corresponds to a more compact and rigid protein conformation, which is probably favorable for stabilizing the protein against alkali-denaturation and suggested to be an important mechanism for structural adaptation of a variety of proteins to alkaline environments[22], [28]. However, it appears that in the alkaline β -mannanases an increase in the number of hydrogen bonds might not be necessary for their enhanced resistance to alkaline pH. Perhaps, increased hydrogen bonding is a favorable but non-essential strategy used by some proteins for alkaline tolerance.

Protein surface

The surface of a protein constitutes the interface through which a protein senses its environment[29]. Extremozymes employ a series of protective strategies to adapt to different extreme conditions, and one of these strategies is changing the content of surface amino acids.

Similar to alkaline xylanases from *Bacillus* sp. N27 and *Bacillus halodurans* S7, BSP165 MAN and its alkaline homologues have more abundant surface-accessible negatively charged residues when compared with the nonalkaline counterparts. Protein surfaces rich in acidic residues probably play an essential role in maintaining protein function under alkaline conditions. Generally, acidic residues exhibit a strong water binding capacity in the deprotonated state at high pH[30] and the presence of numerous negatively charged carboxylates on the surface of a protein can keep the protein completely hydrated, thus preventing it from aggregating[31]. In addition, numerous surface-exposed negatively charged carboxylates might help protect the protein core from OH⁻ attack, stabilizing the protein under alkaline conditions[32].

There are also significant differences in the total number of polar residues on the surface between alkaline and nonalkaline ones, especially in the number of Ser and Thr residues. Since an excess of polar residues on the protein surface might disturb the local stability at higher pH due to their unstable physical-chemical properties, the absence of these residues might help to maintain the balance.

Active site

In general, the pH-activity profile of retaining glycosyl hydrolases is governed by the pK_a values of the proton donor and the catalytic nucleophilic residue [33], [34], [35], [36], [37]. Some key residues in the vicinity of the active site, directly or indirectly interacting with the catalytic carboxylates, can affect the

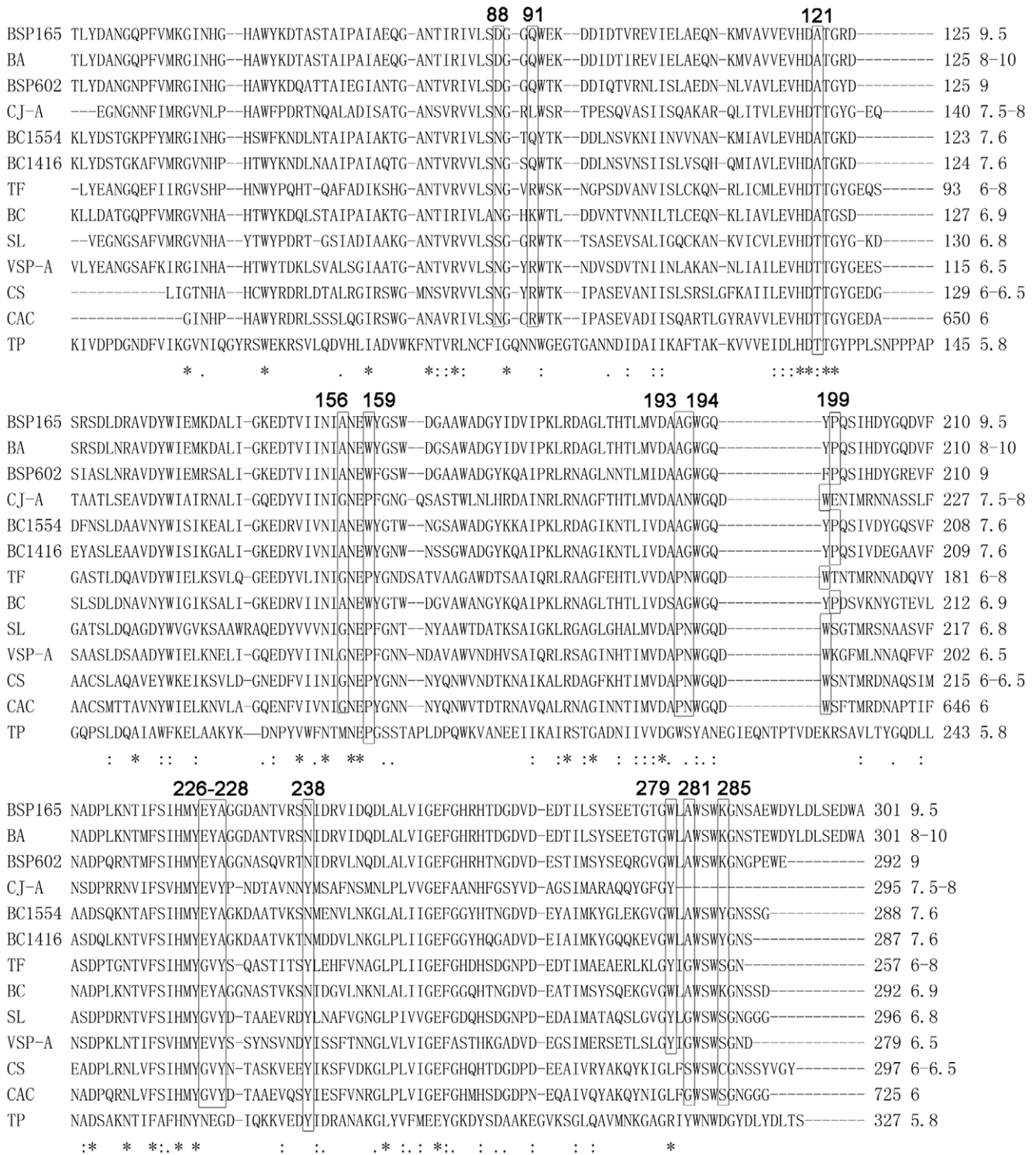


Figure 3. Multiple sequence alignment of GH5-8 mannanases that pH-dependent activities have been characterized. Amino acid residues possibly responsible for the different pH-related activities are labeled. The numbers following the amino acid number indicate the pH optimum.
doi:10.1371/journal.pone.0014608.g003

pK_a values of the catalytic residues by changing the electrostatic and/or dynamic aspects of the active site[38], and are at least partially responsible for the different pH-dependent activities of homologous enzymes[39], [40]. Identification of key residues based on comparisons with homologous enzyme that possesses

obvious distinct pH-activity profile has been proven effective. Thus, 15 residues within a radius of 12 Å from either of the two catalytic amino acids in BSP165 and TF MAN were selected based on structural and homologous sequences alignment. We calculated the achievable ΔpK_a values for two target titratable groups in

Table 4. Calculated changes of pK_a values and pH optima of the mutant BSP165 and TF MAN.

Mutant		ΔpK_a (proton donor)		ΔpK_a (catalytic base)		ΔpH_{opt}	
BSP165	TF	ΔpK_a (E158)	ΔpK_a (E128)	ΔpK_a (E253)	ΔpK_a (E225)	BSP165	TF
D88N	N55D	-0.159	0.039	0.018	-0.011	-0.07	0.014
Q91R	R58Q	-0.464	0.542	-0.411	0.437	-0.438	0.4895
A121T	T88A	0.005	0.152	0.025	0.082	0.015	0.117
A156G	G126A	-0.088	-0.001	0.026	-0.033	-0.031	-0.017
W159P	P129W	-0.114	0.099	-0.019	0	-0.066	0.0495
A193P	P165A	-0.086	0.053	-0.071	0.014	-0.079	0.0335
G194N	N166G	-0.184	0.044	-0.071	0.061	-0.128	0.0525
P199W	W171P	-0.014	0.038	-0.038	0.081	-0.026	0.0595
E226G	G199E	-0.898	0.378	-0.049	-0.055	-0.474	0.1615
Y227V	V200Y	-0.061	0.022	-0.1	-0.01	-0.081	0.006
A228Y	Y201A	-0.058	-0.007	-0.008	0.084	-0.033	0.0385
N238Y	Y210N	-0.068	-0.048	-0.094	-0.051	-0.081	-0.0495
W279Y	Y251W	-0.047	0.01	0.094	0.017	0.0235	0.0135
A281G	G253A	-0.013	0.006	-0.003	-0.031	-0.008	-0.0125
K285S	S257K	-0.016	-0.043	0.054	-0.113	0.019	-0.078

doi:10.1371/journal.pone.0014608.t004

BSP165 and TF MAN by introducing reciprocal mutations. The results showed mutations at amino acid sites Q91 and E226 (numbering based on BSP165 MAN) significantly changed pK_a values in both enzymes to opposite direction as deduced. Further, pH-activity profiles of mutants at position 91 and 226 were analyzed. The direction of the pH-activity profile shifts for BSP165 MAN mutants are reproduced well by the pK_a calculations. Especially the double mutation at the two sites has shown a substantially decreased activity in the alkaline range (Figure 4). These experimental data have proved these two sites are important for high pH catalysis of BSP165 MAN. This would mean that mutations at amino acid sites Q91 and E226 (numbering based on BSP165 MAN) might be involved in an evolutionarily critical change in the pH optimum for GH5-8 mannanases.

Gln91 is situated in a loop connecting β -stand 2 and α -helix 2 of the TIM-barrel. Its distances from the target groups are 11.50 Å (Glu158 C δ) and 14.06 Å (Glu253 C δ), respectively (Figure 5). Probably, the mutation Q91R brings the electrostatic changes to the active site by introducing a positive charge and in this way perturbing the pK_a values of the active site acids. Glu226 sits in the loop that covers the active site and is next to Tyr225, one of the eight conserved amino acids in GH5-8 mannanases (Figure 5). Changes of the solvent accessibility and the dynamics of Tyr225 introduced by the mutation of E226G might perturb the stabilization of the active-site environment and influence the protonation state of the catalytic glutamate residues. We speculate that the pH-activity profile shift is a combined effect of the charge and the change in mobility of Tyr225 that are induced by mutation of E226G. However, the magnitude of the pH-activity profile shifts is not well reproduced, especially for E226G. The discrepancy is not readily explainable and is possibly due to changes in stability.

In conclusion, the crystal structure of the catalytic domain of mannanase from alkaliphilic *Bacillus* sp. N16-5, BS165 MAN, has been determined at 1.6 Å resolution. In order to illustrate molecular mechanism for alkaline adaptation in GH5 β -

mannanases, thorough comparisons were carried out and several distinctive structural features were identified. In mannanases active at elevated pH, an increase in the hydrophobic residues and Arg residue content and a decrease in polar residues were observed on the level of primary structure comparison. Besides, changes in the position and length of helices, strands and loops were found, which might contribute to subtle influence on the catalytic environment, thus affecting the pH-dependent properties. Negatively charged residues were favored on the surface of alkaline mannanases, as reported for other alkaline active enzymes, at the expense of polar residues. pK_a calculations and analysis of mutant mannanases further revealed that the location of Gln91 and Glu226 render BSP165 MAN active under high pH conditions, and mutations at the two sites might be involved in an evolutionarily critical change in the pH optimum for the activity of GH5-8 mannanases. Our analysis would help to engineer proteins with improved stability and activity in alkaline conditions, a requirement for biotechnological applications.

Materials and Methods

Crystallization, data collection, structure resolution and refinement

The purification, crystallization and data collection of the catalytic domain of the enzyme were carried out as previously described [16]. Briefly, crystals with average dimensions of $50 \times 100 \times 200 \mu\text{m}$ were obtained at 25°C in 2–3 days by setting up 2 μl crystallization drops containing 0.5 M $(\text{NH}_4)_2\text{SO}_4$, 0.1 M sodium-citrate (pH 5.6), 1.2 M Li_2SO_4 and 2.0 mg ml^{-1} protein. The structure was solved by the molecular replacement method with the program MOLREP [41] from the CCP4 program package [42], using the crystal structure of the β -mannanase from alkaliphilic *Bacillus* sp. JAMB-602 (PDB code 1WKY) as the search model. There is one molecule in the asymmetric unit that corresponds to the Matthews coefficient [43] of $2.36 \text{ \AA}^3 \text{ Da}^{-1}$. Refinement was carried out using the parameters of Engh and Huber [44] and model building was carried out using Phenix

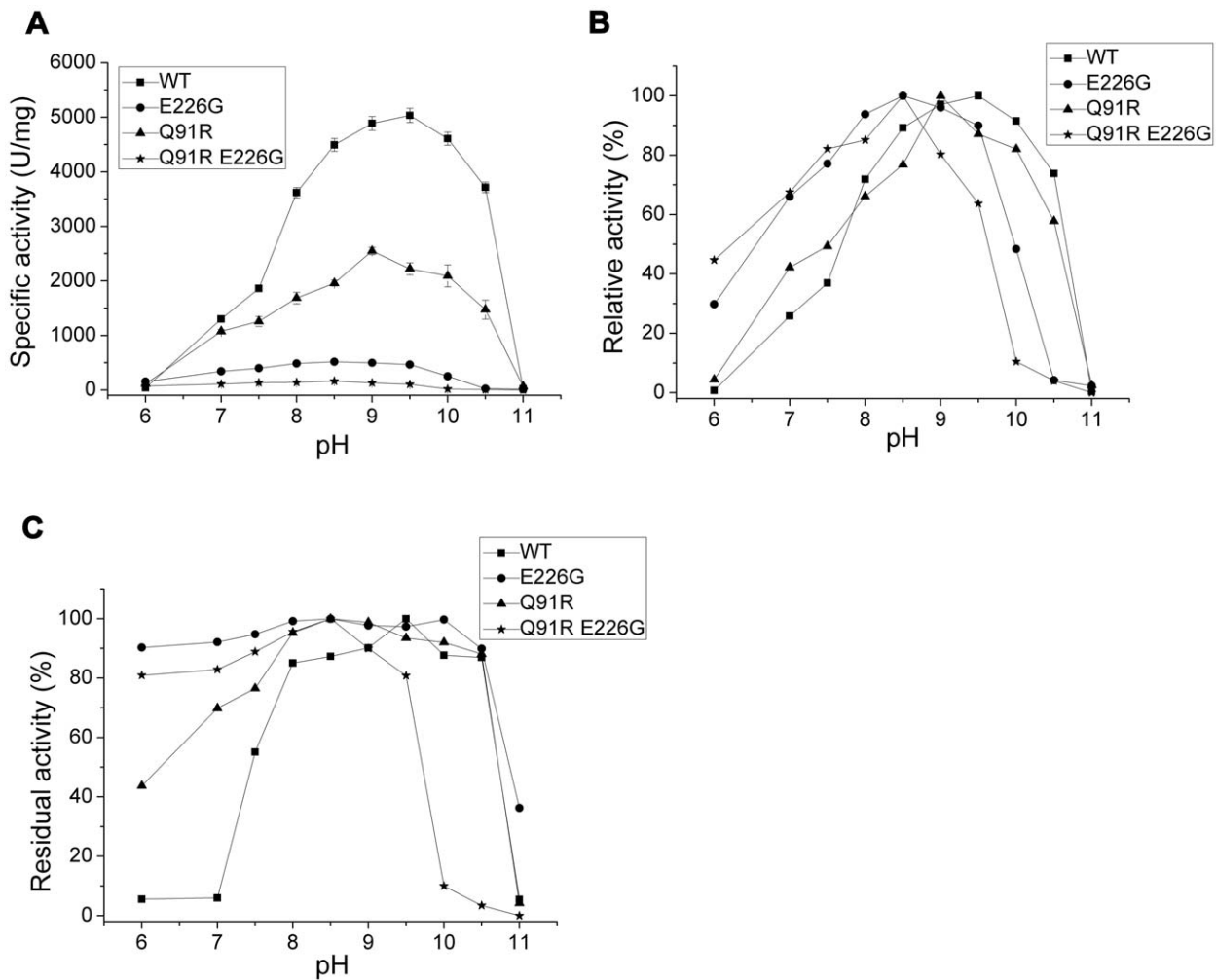


Figure 4. Effect of pH on the activity and stability of wild type and the mutant BS165 MAN. A: pH-dependent specific activity. B: pH-dependent relative activity. C: pH stability. Wild type (■), Q91R (▲), E226G (●) and Q91R E226G (★). doi:10.1371/journal.pone.0014608.g004

(1.3)[45]. Five percent of randomly selected observed reflections were kept aside for the cross-validation. The stereochemistry of the final models was analyzed with PROCHECK[46], and RMSD resulted in the proper values (Table 1).

Phylogenetic analysis

The characterized family 5 β -mannanases were selected referring to http://www.cazy.org/GH5_characterized.html. The ClustalW program[47] was used for multiple sequence alignment of amino acid sequences. Sequences encoding their catalytic domains were retrieved from the GenBank database based on the notation in the features. Phylogenetic tree was constructed with the neighbor-joining method[48] and the minimum evolution method[49], both from MEGA software version 3.1[50]. The p-distance and Poisson correction substitution models were used in both tree-building methods. Bootstrap values were calculated based on 1,000 replicates of the data[51].

Comparison with other family 5 β -mannanases

The total amino acid compositions of the catalytic domains were calculated with MEGA software version 3.1. The two-sample

Student's *t*-value was then calculated using PASW statistics 18 (SPSS Inc., Chicago, Illinois).

Structural analysis

The solvent-exposed residues were identified using the cutoff value of $\geq 30\%$ for the relative surface accessibility area of the side chain in Swiss-PDB Viewer[52] using the default probe radius. Hydrogen bonds and contacts were assessed by HBPLUS[53]. Secondary structure elements were analyzed with DSSP[54]. Structure-based alignment was performed using ESPript[55]. Molecule figures were created using PyMOL (Delano Scientific LLC, Palo Alto, CA, USA). Compactness coefficient is defined as the ratio of the accessible surface area of a protein to that of the ideal sphere of the same volume[56].

pK_a calculations

The pK_a of ionizable groups were predicted by using MCCE version 2.4[57], [58], [59]. MCCE uses the DelPhi program version 4[60]. The parameters were set as follows: ionic strength 0.05 M, initial pH = 3.0, titration points 60 and other default values.

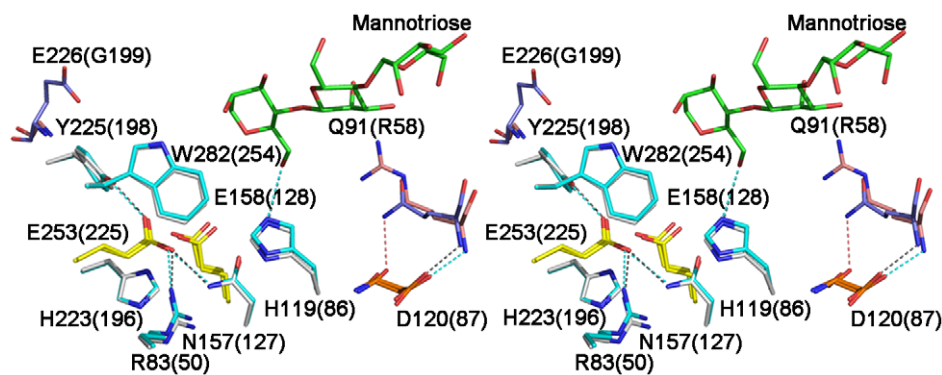


Figure 5. Stereo view of two point mutation sites around the catalytic center in BSP165 MAN (Q91 and E226, shown in blue) and TF MAN (R58 and G199, shown in pink). Hydrogen bonds are represented by dashed lines. Mannotriose bound to TF MAN is shown in green. doi:10.1371/journal.pone.0014608.g005

A model of BSP165 MAN in complex with mannotriose was constructed from the TF Man- mannotriose X-ray structure[17].

Preparation of mutant structures

Mutant structures for pK_a calculations were designed using backbone dependent rotamer library[61].

Mutagenesis and enzyme preparation

Site-directed mutagenesis was performed using the QuikChange Site-Directed Mutagenesis Kit (Stratagene) and the recombinant vector pETMAN330[16] containing the gene encoding the catalytic domain as a template. The codon for Gln91 (CAA) was replaced with AGA (Q91R) and the codon for Glu226 (GAG) with GGG (E226G). The mutant genes were sequenced to confirm the mutations. The wild type and mutant proteins were expressed and purified as described by Zhao *et al.*[16]. The protein purities were checked by SDS-PAGE[62] stained with Coomassie Brilliant Blue. The protein concentration was measured with a protein assay kit (Bio-Rad, USA), with BSA as a standard.

Enzyme assay

The catalytic activity of the purified recombinant wide-type and mutant β -mannanases were determined using locust bean gum as substrate according to the procedure described previously[11]. Buffers, 0.05 M $\text{Na}_2\text{HPO}_4\text{-NaH}_2\text{PO}_4$ (pH 6.0–7.5), 0.05 M Tris-HCl (pH 7.5–8.5), 0.05 M Glycyl-NaOH (pH 8.5–10.5) and 0.05 M $\text{Na}_2\text{HPO}_4\text{-NaOH}$ (pH 11–12) were used. Stability was determined as the residual activity after incubation at 50°C in 50 mM buffers for 1 hour.

Since the substrate is insoluble in water (and added in large quantities), the activity measurements obtained by this method can be regarded as a k_{cat} for insoluble locust bean gum.

Protein Data Bank accession codes

Atomic coordinates and structure factors have been deposited with the Protein Data Bank entry code 3JUG.

Supporting Information

Table S1 All pH-dependent activity characterized β -mannanases from GH5.

References

- Ito S, Kobayashi T, Ara K, Ozaki K, Kawai S, et al. (1998) Alkaline detergent enzymes from alkaliphiles: enzymatic properties, genetics, and structures. *Extremophiles* 2: 185–190.
- Horikoshi K (1999) Alkaliphiles: Some applications of their products for biotechnology. *Microbiology and Molecular Biology Reviews* 63: 735–750.

Found at: doi:10.1371/journal.pone.0014608.s001 (0.10 MB DOC)

Table S2 Comparison of BSP165 MAN with other 3D structure-known β -mannanases of GH5.

Found at: doi:10.1371/journal.pone.0014608.s002 (0.05 MB DOC)

Figure S1 Phylogenetic tree showing the relationship between BSP165 MAN and other characterized GH5 β -mannanases. Numbers at nodes represent the levels of bootstrap support (%) based on a neighbor-joining analysis of 1000 resampled datasets. The bar indicates a branch length equivalent to 0.2 changes per amino acid. The numbers following the enzyme abbreviations (listed in table S1) indicate the pH optima.

Found at: doi:10.1371/journal.pone.0014608.s003 (0.11 MB TIF)

Figure S2 Overall structures (TIM barrel) representation of BSP165 (A), BA (B), BSP602 (C), TF (D), HJ (E) and ME MAN (F). The different views are indicated as i (top view) and ii (side view). The arrow indicates where the catalytic cleft is positioned in a $(\beta\alpha)_8$ -barrel fold.

Found at: doi:10.1371/journal.pone.0014608.s004 (1.81 MB TIF)

Figure S3 A: Stereo view of superimposition of BSP165 MAN (cyan) with BA (yellow), BSP602 (magenta) and TF (green) MAN in the catalytic site. B: Stereo view of superimposition of BSP165 MAN (cyan) with HJ MAN (pink) in the catalytic site. C: Stereo view of superimposition of BSP165 MAN (cyan) with ME MAN (gray) in the catalytic site.

Found at: doi:10.1371/journal.pone.0014608.s005 (0.56 MB TIF)

Acknowledgments

We are very grateful to Yang Liu and Ruiting Guo for their extensive help.

Author Contributions

Conceived and designed the experiments: Y Zhao YX YM. Performed the experiments: Y Zhao Y Zhang LM. Analyzed the data: Y Zhao YC JQ FG HP. Contributed reagents/materials/analysis tools: Y Zhao YC JQ FG HP XW GFG. Wrote the paper: Y Zhao YX YM.

3. Horikoshi K (2004) Alkaliphiles. Proceedings of the Japan Academy Series B-Physical and Biological Sciences 80: 166–178.
4. McCleary BV (1983) Beta-D-Mannosidase from *Helix pomatia*. Carbohydrate Research 111: 297–310.
5. Singh S, Madlala AM, Prior BA (2003) *Thermomyces lanuginosus*: properties of strains and their hemicellulases. FEMS Microbiology Reviews 27: 3–16.
6. Dekker RF, Richards GN (1976) Hemicellulases: their occurrence, purification, properties, and mode of action. Advances in Carbohydrate Chemistry and Biochemistry 32: 277–352.
7. Kansoh AL, Nagieb ZA (2004) Xylanase and mannanase enzymes from *Streptomyces galbus* NR and their use in biobleaching of softwood kraft pulp. Antonie Van Leeuwenhoek 85: 103–114.
8. Li Y, Yang P, Meng K, Wang Y, Luo H, et al. (2008) Gene cloning, expression, and characterization of a novel beta-mannanase from *Bacillus circulans* CGMCC 1416. Journal of Microbiology and Biotechnology 18: 160–166.
9. Akino T, Nakamura N, Horikoshi K (1987) Production of β -mannosidase and β -mannanase by an alkalophilic *Bacillus* sp. Applied Microbiology and Biotechnology 26: 323–327.
10. Akita M, Takeda N, Hirasawa K, Sakai H, Kawamoto M, et al. (2004) Crystallization and preliminary X-ray study of alkaline mannanase from an alkaliphilic *Bacillus* isolate. Acta Crystallographica, Section D: Biological Crystallography 60: 1490–1492.
11. Ma Y, Xue Y, Dou Y, Xu Z, Tao W, et al. (2004) Characterization and gene cloning of a novel beta-mannanase from alkaliphilic *Bacillus* sp. N16-5. Extremophiles 8: 447–454.
12. Hatada Y, Takeda N, Hirasawa K, Ohta Y, Usami R, et al. (2005) Sequence of the gene for a high-alkaline mannanase from an alkaliphilic *Bacillus* sp. strain JAMB-750, its expression in *Bacillus subtilis* and characterization of the recombinant enzyme. Extremophiles 9: 497–500.
13. Bettiol JP, Showell MS (2002) US Patent 6: 376–445.
14. Yang P, Li Y, Wang Y, Meng K, Luo H, et al. (2008) A novel beta-mannanase with high specific activity from *Bacillus circulans* CGMCC1554: gene cloning, expression and enzymatic characterization. Applied Biochemistry and Biotechnology. pp 1559–0291.
15. Taillford LE, Ducros VMA, Flint JE, Roberts SM, Morland C, et al. (2009) Understanding How Diverse β -Mannanases Recognize Heterogeneous Substrates. Biochemistry 48: 7009–7018.
16. Zhao Y, Zhang Y, Gao F, Xue Y, Zeng Y, et al. (2008) Crystallization and preliminary X-ray study of alkaline beta-mannanase from the alkaliphilic *Bacillus* sp. N16-5. Acta Crystallographica, Section F: Structural Biology and Crystallization Communications 64: 957–959.
17. Hilge M, Gloor SM, Rypniewski W, Sauer O, Heightman TD, et al. (1998) High-resolution native and complex structures of thermostable beta-mannanase from *Thermomonospora fusca* substrate specificity in glycosyl hydrolase family 5. Structure 6: 1433–1444.
18. Xu B, Hagglund P, Stalbrand H, Janson JC (2002) endo-beta-1,4-Mannanases from blue mussel, *Mytilus edulis*: purification, characterization, and mode of action. Journal of Biotechnology 92: 267–277.
19. Larsson AM, Anderson L, Xu B, Munoz IG, Uson I, et al. (2006) Three-dimensional crystal structure and enzymic characterization of beta-mannanase Man5A from blue mussel *Mytilus edulis*. Journal of Molecular Biology 357: 1500–1510.
20. Stalbrand H, Siika-aho M, Tenkanen M, Viikari L (1993) Purification and characterization of two β -mannanases from *Trichoderma reesei*. Journal of Biotechnology 29: 229–242.
21. Sabini E, Schubert H, Murshudov G, Wilson KS, Siika-Aho M, et al. (2000) The three-dimensional structure of a *Trichoderma reesei* beta-mannanase from glycoside hydrolase family 5. Acta Crystallographica, Section D: Biological Crystallography 56: 3–13.
22. Shirai T, Suzuki A, Yamane T, Ashida T, Kobayashi T, et al. (1997) High-resolution crystal structure of M-protease: phylogeny aided analysis of the high-alkaline adaptation mechanism. Protein Engineering, Design and Selection 10: 627–634.
23. Shirai T, Ishida H, Noda J, Yamane T, Ozaki K, et al. (2001) Crystal structure of alkaline cellulase K: insight into the alkaline adaptation of an industrial enzyme. Journal of Molecular Biology 310: 1079–1087.
24. Shirai T, Igarashi K, Ozawa T, Hagihara H, Kobayashi T, et al. (2007) Ancestral sequence evolutionary trace and crystal structure analyses of alkaline alpha-amylase from *Bacillus* sp KSM-1378 to clarify the alkaline adaptation process of proteins. Proteins: Structure, Function, and Bioinformatics 66: 600–610.
25. Mamo G, Thunnissen M, Hatti-Kaul R, Mattiasson B (2009) An alkaline active xylanase: insights into mechanisms of high pH catalytic adaptation. Biochimie 91: 1187–1196.
26. Besir H, Zeth K, Bracher A, Heider U, Ishibashi M, et al. (2005) Structure of a halophilic nucleoside diphosphate kinase from *Halobacterium salinarum*. FEBS Letters 579: 6595–6600.
27. Fang TY, Ford C (1998) Protein engineering of *Aspergillus awamori* glucoamylase to increase its pH optimum. Protein Engineering 11: 383–388.
28. Dubnovitsky AP, Kapetanios EG, Papageorgiou AC (2005) Enzyme adaptation to alkaline pH: Atomic resolution (1.08Å) structure of phosphoserine aminotransferase from *Bacillus alcalophilus*. Protein Science 14: 97–110.
29. Neves Petersen MT, Fojan P, Petersen SB (2001) How do lipases and esterases work: the electrostatic contribution. Journal of Biotechnology 85: 115–147.
30. Kuntz ID (1971) Hydration of macromolecules. III Hydration of polypeptides. Journal of the American Chemical Society 93: 514–516.
31. Fushinobu S, Ito K, Konno M, Wakagi T, Matsuzawa H (1998) Crystallographic and mutational analyses of an extremely acidophilic and acid-stable xylanase: biased distribution of acidic residues and importance of Asp37 for catalysis at low pH. Protein Engineering 11: 1121–1128.
32. Manikandan K, Bhardwaj A, Gupta N, Lokanath NK, Ghosh A, et al. (2006) Crystal structures of native and xylosaccharide-bound alkali thermostable xylanase from an alkaliphilic *Bacillus* sp. NG-27: structural insights into alkaliphilicity and implications for adaptation to polyextreme conditions. Protein Science 15: 1951–1960.
33. Antosiewicz J, McCammon JA, Gilson MK (1994) Prediction of pH-dependent properties of proteins. Journal of Molecular Biology 238: 415–436.
34. Kim JR, Yang JH, Young JY (2002) The optimum pH of oxidoreductases: a comparison between experimental and calculated pH optimum. Journal of the Korean Chemical Society 46: 432–436.
35. Nielsen JE, McCammon JA (2003) Calculating pKa values in enzyme active sites. Protein Science 12: 1894–1901.
36. Yang AS, Honig B (1993) On the pH dependence of protein stability. Journal of Molecular Biology 231: 459–474.
37. Yang JH, Park JY, Kim SH, Yoo YJ (2008) Shifting pH optimum of *Bacillus circulans* xylanase based on molecular modeling. Journal of Biotechnology 133: 294–300.
38. Nielsen JE, Borchert TV, Vriend G (2001) The determinants of alpha-amylase pH-activity profiles. Protein Engineering 14: 505–512.
39. Coughlan S, Wang XG, Britton KL, Stillman TJ, Rice DW, et al. (2001) Contribution of an aspartate residue, D114, in the active site of clostridial glutamate dehydrogenase to the enzyme's unusual pH dependence. Biochimica et Biophysica Acta 1544: 10–17.
40. Lee SJ, Lee DW, Choe EA, Hong YH, Kim SB, et al. (2005) Characterization of a thermoacidophilic L-arabinose isomerase from *Alcalyobacillus acidocaldarius*: role of Lys-269 in pH optimum. Applied and Environmental Microbiology 71: 7888–7896.
41. Vagin A, Teplyakov A (1997) MOLREP: an Automated Program for Molecular Replacement. Journal of Applied Crystallography 30: 1022–1025.
42. Collaborative Computational Project, Number 4 (1994) Acta Crystallographica, Section D: Biological Crystallography 50: 760–763.
43. Matthews BW (1968) Solvent content of protein crystals. Journal of Molecular Biology 33: 491–497.
44. Engh RA, Huber R (1991) Accurate bond and angle parameters for X-ray protein structure refinement. Acta Crystallographica, Section A: Foundations of Crystallography 47: 392–400.
45. Adams PD, Grosse-Kunstleve RW, Hung LW, Ioerger TR, McCoy AJ, et al. (2002) PHENIX: building new software for automated crystallographic structure determination. Acta Crystallographica Section D: Biological Crystallography 58: 1948–1954.
46. Laskowski RA, MacArthur MW, Moss DS, Thornton JM (1993) PROCHECK: a program to check the stereochemical quality of protein structures. Journal of Applied Crystallography 26: 283–291.
47. Thompson JD, Higgins DG, Gibson TJ (1994) CLUSTAL W: improving the sensitivity of progressive multiple sequence alignment through sequence weighting, position-specific gap penalties and weight matrix choice. Nucleic Acids Research 22: 4673–4680.
48. Saitou N, Nei M (1987) The neighbor-joining method: a new method for reconstructing phylogenetic trees. Molecular Biology and Evolution 4: 406–425.
49. Rzhetsky A, Nei M (1993) Theoretical foundation of the minimum-evolution method of phylogenetic inference. Molecular Biology and Evolution 10: 1073–1095.
50. Kumar S, Tamura K, Nei M (2004) MEGA3: Integrated software for Molecular Evolutionary Genetics Analysis and sequence alignment. Briefings in Bioinformatics 5: 150–163.
51. Felsenstein J (1996) Inferring phylogenies from protein sequences by parsimony, distance, and likelihood methods. Methods in Enzymology 266: 418–427.
52. Guex N, Peitsch MC (1997) SWISS-MODEL and the Swiss-PdbViewer: an environment for comparative protein modeling. Electrophoresis 18: 2714–2723.
53. McDonald IK, Thornton JM (1994) Satisfying hydrogen bonding potential in proteins. Journal of Molecular Biology 238: 777–793.
54. Kabsch W, Sander C (1983) Dictionary of protein secondary structure: pattern recognition of hydrogen-bonded and geometrical features. Biopolymers 22: 2577–2637.
55. Gouet P, Courcelle E, Stuart DI, Metz F (1999) ESPript: analysis of multiple sequence alignments in PostScript. Bioinformatics 15: 305–308.
56. Galzitskaya OV, Bogatyreva NS, Ivankov DN (2008) Compactness determines protein folding type. J Bioinform Comput Biol 6: 667–680.
57. Song Y, Mao J, Gunner MR (2009) MCCE2: improving protein pKa calculations with extensive side chain rotamer sampling. Journal of Computational Chemistry 30: 2231–2247.
58. Georgescu RE, Alexov EG, Gunner MR (2002) Combining conformational flexibility and continuum electrostatics for calculating pK(a)s in proteins. Biophysical Journal 83: 1731–1748.
59. Alexov EG, Gunner MR (1997) Incorporating protein conformational flexibility into the calculation of pH-dependent protein properties. Biophysical Journal 72: 2075–2093.

60. Alexov E, Honig B (2001) Extending the Applicability of the Nonlinear Poisson-Boltzmann Equation: Multiple Dielectric Constants and Multivalent Ions. *The Journal of Physical Chemistry B* 105: 6507–6514.
61. Dunbrack RL, Jr., Cohen FE (1997) Bayesian statistical analysis of protein side-chain rotamer preferences. *Protein Science* 6: 1661–1681.
62. Laemmli UK (1970) Cleavage of structural proteins during the assembly of the head of bacteriophage T4. *Nature* 227: 680–685.